Volume 1 | Number 1 | Jan 2013 | Pages 1–100

ChemComm

Chemical Communications
www.rsc.org/chemcomm

ROYAL SOCIETY
OF CHEMISTRY

ROYAL SOCIETY
OF CHEMISTRY

www.rsc.org/chemcomm

Journal Name

ChemComm

ARTICLE TYPE

Hollow Iron Oxide Nanoshells are Active and Selective Catalysts for the Partial Oxidation of Styrene with Molecular Oxygen

**Monika Joanna Rak,** [a] **Michael Lerro,** [a] **and Audrey Moores*** [a]

Well defined hollow iron oxide nanoshells are active, selective and recyclable catalysts for the oxidation of styrene into benzaldehyde using the difficult-to-activate molecular oxygen as the sole oxidant. Using no noble metals, unprecedented
10 **conversion of 90% was maintained while high selectivity of 73% was able to be achieved.**

Outdone only by vanillin (vanilla aroma), benzaldehyde (almond aroma) is the second most used flavouring agent.[1] In 2009, it was
15 estimated that 90 kilotons[2] of benzaldehyde were synthesized through industrial processes hampered by high temperatures and pressures that nevertheless resulted in lackluster yields.[3] One industrial pathway to benzaldehyde is the hydrolysis of benzal chloride synthesis which generates large quantities of HCl as a
20 by-product.[4] The alternative, and more popular industry method of air-oxidation of toluene, results in low conversions of starting materials and produces benzaldehyde only as a by-product in the production of the less valuable benzoic acid.[3, 5]
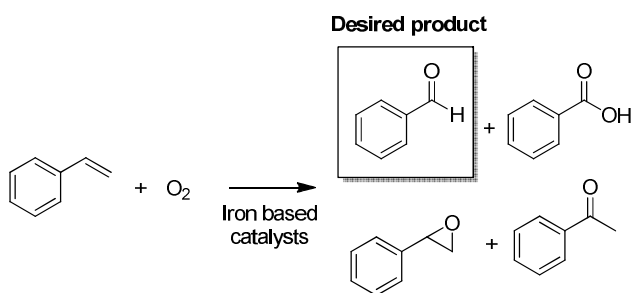
Scheme 1 Styrene oxidation using molecular oxygen as oxidant. Reaction
25 conditions: 0.5 mol % catalyst, 4bar O_2, 24h, acetonitrile.

Due to the inherent advantages of using molecular oxygen being cheap, readily available, and ensuring a high atom economy, there has recently been an increased interest in the
30 oxidation of styrene using molecular oxygen to produce benzaldehyde.[6] Despite these advantages, it remains a challenge to use molecular oxygen effectively for partial oxidations of olefins to aldehydes while limiting the production of carboxylic acids. Work done using homogeneous noble metal-based systems
35 has shown some success for this task. Feng *et al.* demonstrated that a Pd(II) complex allowed excellent conversions and selectivities as well as good recyclability.[7] On the other hand, heterogeneous supported gold nanoparticle (AuNP) catalysts have garnered a lot of attention for oxidation reactions[8] and in 2008,
40 Lambert and coworkers showed that titania supported $Au_{55}NP$ were able to effect conversions of styrene to benzaldehyde under particularly mild conditions using molecular oxygen.[9] More recently, $Pt@Fe_2O_3$[10] and gold[11] nanowires also demonstrated oxidative activity under mild conditions. These catalysts feature
45 good selectivity for benzaldehyde (94%) with poor yields (<10%). When the conversions are pushed, selectivity drops dramatically. These heterogeneous catalysts unfortunately suffered from poor recyclability with both activity and selectivity falling upon reuse of the catalyst.
50 Iron oxide, meanwhile, has long demonstrated a high efficiency as an effective catalyst for a variety of oxidation reactions[12-15] because it is cheap, nontoxic, and earth abundant, making it an attractive material in the context of green chemistry. Furthermore, when in the form of NPs, iron oxide can be
55 recovered magnetically.[16, 17] Most examples are concerned with the use of hydrogen peroxide to oxidize aryl double bonds and alcohols.[12, 15] Notably, Beller and coll. demonstrated that benzaldehyde could be obtained with high conversion and selectivity from benzyl alcohol; aryl alkenes were also converted
60 with high selectivities although with modest conversions (<50%).[12] More recently, Luque and coworkers used mesoporous silica supported iron oxide to convert styrene to benzaldehyde with high yield with H_2O_2 as the oxidant.[18]

We decided to study the activity of iron oxide nanoparticles,
65 without the aid of noble metals, for the selective oxidation of styrene to benzaldehyde using molecular oxygen as the sole oxidant (Scheme 1). Previous work has shown that a decrease in size of iron NPs results in an increased conversion but a decreased selectivity.[12, 13] We chose to investigate the effect of
70 an interesting feature of NPs, namely their ability to produce hollow nanoshells, on the conversion and selectivity for oxidation of styrene to benzaldehyde. Although several syntheses exist for making hollow iron oxide nanoparticle structures,[19] their application in catalysis has been little studied. Hollow iron oxide
75 structures for oxidations have been attempted in 2011, by Zhang *et al.* who studied α-Fe_2O_3 nanotubes in a photocatalytic oxidation of naphthalene to produce CO_2, CO, H_2O, and phthalic anhydride.[20] In the present work, we compared hollow ferrite nanoshells (Fe_3O_4 NS), as well as etched Fe_3O_4 NS, to solid
80 ferrite and ferrous oxide NPs and reduced iron NPs for the partial oxidation of styrene (Scheme 2). The results presented herein

show that Fe_3O_4 NS and their etched counterparts successfully combined high selectivity to high activity for the very attractive synthesis of benzaldehyde from styrene and O_2.

Tested iron-based catalysts:

| Fe_2O_3 NP | Fe_3O_4 NP | Fe/FeOC/S | Fe_3O_4 NS | eFe_3O_4 NS |
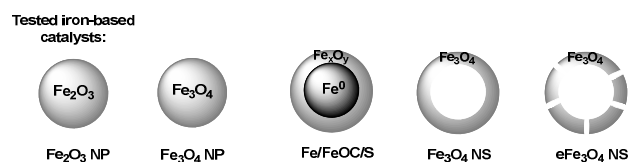
5   Scheme 2: Catalysts tested in this work

Fe_2O_3 and Fe_3O_4 NPs were purchased from Sigma Aldrich and used as received. Fe/Fe_xO_y core/shell NP (Fe/FeOC/S) were synthesized using the reduction of $Fe(SO_4)$ in water using a previously reported procedure.[21, 22] Iron oxide nanoshells (Fe_3O_4
10 NS) were synthesised through oxidation of Fe(0) NPs by air at 260°C, following a method reported by Sun and co-workers (Figure 1).[23] In a typical reaction, 5mg of the catalyst were loaded with 4.75g of styrene in acetonitrile (1.8M solution) at 90°C with 4bar of O_2 for 24 hours (Table 1).[‡] This reaction afforded 4
15 products: benzaldehyde, benzoic acid, acetophenone and styrene oxide (Scheme 1). The catalysts were probed for their conversion and selectivity towards benzaldehyde formation. The latter criterion was high (78 to 81%) for Fe_2O_3, Fe_3O_4 NPs and Fe/FeOC/S, but associated with moderate conversions between
20 49 and 56% in all cases. Interestingly, Fe_3O_4 NS afforded a much improved conversion of 84%, while the selectivity was eroded but maintained at a high level of 65%. These results clearly evidenced that Fe_3O_4 NS are more active for the reaction of oxidation and the slight drop in selectivity compared to non-
25 hollow counterparts could be attributed to conversion to benzoic acid.

Various conditions were tested with Fe_3O_4 NS. Running the reaction neat or in water resulted in styrene polymerizing. Toluene showed similar trends to acetonitrile, but with reduced
30 conversions (Table S1). Temperature optimization reactions were attempted with this solvent at two pressures; one at 4bar (Table S2) and one at 30bar (Table S3) of O_2 in toluene. The reaction was book-ended by temperatures which on the low end gave no reaction and on the high end resulted in polymerization.
35 Increasing the pressure resulted in the undesirable production of more benzoic acid.

In order to better understand the unique reactivity of Fe_3O_4 NS, the complete characterization of this nanomaterial was undertaken. Fe_3O_4 NS are obtained through rapid oxidation of
40 Fe(0) NPs obtained by thermal decomposition of $Fe(CO)_5$. Transmission electron micrographs (TEM) reveal that the Fe_3O_4 NS are very monodisperse with a size of 16.7±2.0nm and a shell
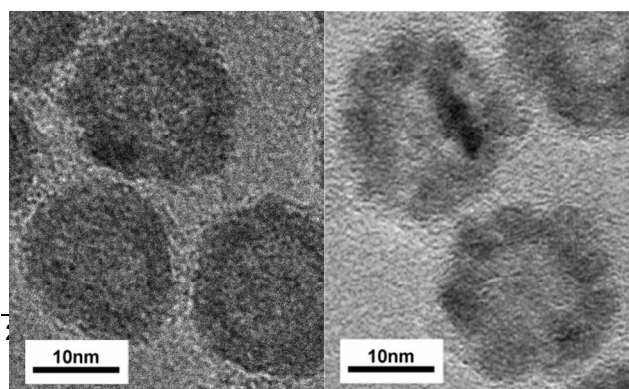
Figure 1: TEM images of Fe_3O_4 NS (left) and eFe_3O_4 NS (right)

of 3.9±0.5nm of thickness. These results are consistent with previous reports.[23] Importantly, the interior hole of the Fe_3O_4 NS
45 is clearly apparent from the images. Some NSs do feature at their centre a small bead of remaining Fe(0) NP (Figure 1, left and S1). The hollow structure is created by Kirkendall effect which forms voids that coalesce in the center of the nanoshell. ICP-MS measurements showed that the heated solution contained less than
50 0.01ppm of dissolved iron, thereby indicating heterogenous catalysis which may be attributed to the surface. To understand whether the catalytic activity is occurring on the exterior or interior surface of the NSs, Brunauer–Emmett–Teller (BET) measurements were performed to determine the presence and
55 potential size of any pores (Figure S2). Surface area measurements show that iron oxide nanoshells to have a specific area of 140 m^2/g. This value is too high to correspond solely to the exterior surface and corresponds to the calculated area of both the exterior and interior surface. This indicates that hollow iron
60 oxide NSs possess a unique chemistry affecting the catalytic properties. The trend of increased catalytic activity for hollow and porous nanoshells relative to solid nanoparticles, has also been reported for gold nanocages, nanoboxes, nanoparticles.[24]

In order to determine how exposing the interior of the iron NS
65 modifies the catalytic behaviour, the NS were etched to afford eFe_3O_4 NS through a process delineated by Sun (Figure S1).[25, 26] This material was used as a drug delivery vehicle. It featured TEM-visible pores (Figure 1, right), which may allow a styrene molecule to enter the interior of the catalyst. Fe_3O_4 NS and
70 eFe_3O_4 NS were compared in optimized conditions, at 4 bar, in acetonitrile and for a range of temperatures from 80 to 100°C (Tables 1, S4, S5). Figure 2 pictures well the trend of decreased selectivity with increased temperature and increased conversion. The etched particles eFe_3O_4 NSs have marginally better
75 selectivity and significantly better conversions (+10-20 point%) over the range of temperatures. The optimal reaction set is obtained for 90°C where conversion of 90% are combined to a high selectivity of 73% for the desired aldehyde product (TON[§]=131.4). This result is unprecedented in terms of
80 selectivity and activity combined for this reaction with O_2. Preliminary kinetic data suggested that eFe_3O_4 NS were able to sustain high selectivities over time in a unique fashion (figure S4). Importantly, these results were obtained in absence of non-noble metal (for comparison see Table S6).
85 As the product has one fewer carbons than the starting material, the fate of the missing carbon was investigated. The cleaved off carbon formed the highly volatile and polymerizable formaldehyde which at lower temperatures could be found as polyacetal solid at the bottom of the reactor. FTIR tests of this
90 undissolvable material revealed a clean spectrum of polyacetal (Figure S3).

eFe_3O_4 NS magnetic properties were exploited to improve the ease and efficiency of removing the catalyst from solution. Discontinuing the stirring allows the NS in solution to settle onto
95 the magnetic stirring bar allowing for the separation of the catalyst from the liquid mixture and its recycling. Throughout 4 consecutive runs, conversion remained high while selectivity dropped off and plateaued. Interestingly, in comparable systems usually both selectivity and activity dropped upon recycling.[9-11]
100 TEM imaging of the eFe_3O_4 NS after 1 and 2 recycle runs

revealed they undergo slow dislocation, possibly explaining the loss of selectivity after recycling (Figure S5). Also oleylamine may play an active role in selectivity as shown by others.[5] A recycling catalytic test was run with eFe_3O_4 NS and additional oleylamine, showing that a part of the selectivity could be recovered (table S7). Addition of oleylamine to Fe_3O_4 NPs, however, could not afford the superior activity and selectivity obtained with hollow structures presented herein (table S7).

Table 1: Styrene oxidation: catalyst screening.[a]

Catalyst	Conv.%	Benzal-dehyde[b]	Benzoic Acid[b]	Other[b,c]
Fe_2O_3 NP	49	81	11	8
Fe_3O_4 NP	53	78	8	14
Fe/FeOC/S	56	81	7	12
Fe_3O_4 NS	84	65	22	13
eFe_3O_4_NS	90	73	13	14

[a] Reaction conditions: 0.5 mol % catalyst, 4bar O_2, 24h, 90°C, 1.8M acetonitrile. [b] Selectivity% [c] Sum of acetophenone, styrene oxide, and oligomers.
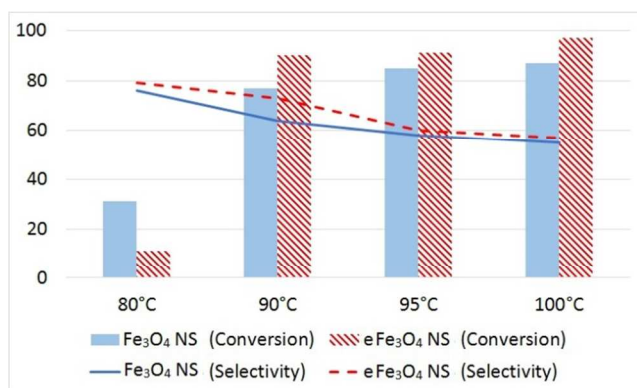

Figure 2: Conversions (clustered columns) and benzaldehyde selectivity (lines) as a function of temperatures with Fe_3O_4 NS (blue, solid) and eFe_3O_4 NS (red, dashed) as catalysts. Reaction conditions: 0.5 mol % catalyst, 4bar O_2, 24h, 1.8M acetonitrile.
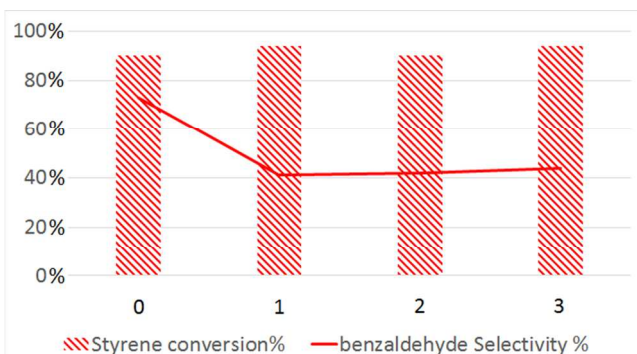

Figure 3: Conversions (clustered columns) and benzaldehyde selectivity (lines) as a function of the number of recycle runs with eFe_3O_4 NS as catalysts. Reaction conditions: 0.5 mol % eFe_3O_4 NS catalyst, 4bar O_2, 24h, 90°C, 1.8M acetonitrile.

In sum, we showed that the porous nature of the hollow iron oxide nanoparticles allowed for a change in catalytic properties, allowing the previously difficult oxidation of styrene with molecular oxygen. Further compelling evidence for the use of hollow iron oxide nanoparticles as a catalyst is that the oxidation process can be controlled to stop at the aldehyde, giving benzaldehyde as the major product.[#]

Notes and references

[a] Centre for Green Chemistry and Catalysis, Department of Chemistry, McGill University, 801 Sherbrooke St West, Montréal, QC H3A 0B8, Canada.. Fax: +1 (514) 398 3797; Tel: +1 (514) 398 4654 E-mail: audrey.moores@mcgill.ca

‡ Octane and dodecane were both used as internal standards to calculate conversion and selectivity percentages via GC-FID.
§ TON=number of moles of aldehyde produced per mole of catalyst[13]

1. U. Krings and R. G. Berger, *Appl. Microbiol. Biotechnol.*, 1998, 49, 1-8.
2. S. Hughes, in *Eur. Chem. Market*, 2010, vol. 44.
3. J. A. B. Satrio and L. K. Doraiswamy, *Chem. Eng. J.*, 2001, 82, 43-56.
4. F. Brühne and E. Wright, in *Ullmann's Encyclopedia of Industrial Chemistry*, Wiley-VCH Verlag GmbH & Co. KGaA, 2000, DOI: 10.1002/14356007.a03_463.
5. J. Lv, Y. Shen, L. Peng, X. Guo and W. Ding, *Chem. Commun.*, 2010, 46, 5909-5911.
6. K. Schröder, B. Join, A. J. Amali, K. Junge, X. Ribas, M. Costas and M. Beller, *Angew. Chem. Int. Ed.*, 2011, 50, 1425-1429.
7. B. Feng, Z. S. Hou, X. R. Wang, Y. Hu, H. Li and Y. X. Qiao, *Green Chem.*, 2009, 11, 1446-1452.
8. M. Haruta, *Nature*, 2005, 437, 1098-1099.
9. M. Turner, V. B. Golovko, O. P. H. Vaughan, P. Abdulkin, A. Berenguer-Murcia, M. S. Tikhov, B. F. G. Johnson and R. M. Lambert, *Nature*, 2008, 454, 981-U931.
10. H. Y. Hong, L. Hu, M. Li, J. W. Zheng, X. H. Sun, X. H. Lu, X. Q. Cao, J. M. Lu and H. W. Gu, *Chem. Eur. J.*, 2011, 17, 8726-8730.
11. L. Hu, X. Cao, J. Yang, M. Li, H. Hong, Q. Xu, J. Ge, L. Wang, J. Lu, L. Chen and H. Gu, *Chem. Commun.*, 2011, 47, 1303-1305.
12. F. Shi, M. K. Tse, M. M. Pohl, J. Radnik, A. Bruckner, S. M. Zhang and M. Beller, *J. Mol. Catal. A: Chem*, 2008, 292, 28-35.
13. F. Shi, M. K. Tse, M. M. Pohl, A. Bruckner, S. M. Zhang and M. Beller, *Angew. Chem. Int. Ed.*, 2007, 46, 8866-8868.
14. K. Schröder, K. Junge, B. Bitterlich and M. Beller, *Top. Organomet. Chem.*, 2011, 33, 83-109.
15. C. González-Arellano, J. M. Campelo, D. J. Macquarrie, J. M. Marinas, A. A. Romero and R. Luque, *ChemSusChem*, 2008, 1, 746-750.
16. V. Polshettiwar and R. S. Varma, *Green Chem.*, 2010, 12, 743-754.
17. R. Hudson, Y. Feng, R. S. Varma and A. Moores, *Green Chem.*, 2014, DOI:10.1039/C1034GC00418C.
18. F. Rajabi, N. Karimi, M. R. Saidi, A. Primo, R. S. Varma and R. Luque, *Adv. Synth. Catal.*, 2012, 354, 1707-1711.
19. K. Cheng, S. Peng, C. Xu and S. Sun, *J. Am. Chem. Soc.*, 2009, 131, 10637-10644.
20. W. H. Zhang, X. Y. Li, Q. D. Zhao, Y. Hou, Y. Shen and G. H. Chen, *Mater. Chem. Phys.*, 2011, 129, 683-687.
21. C. M. Cirtiu, T. Raychoudhuty, S. Ghoshal and A. Moores, *Colloids Surf., A*, 2011, 390, 95-104.
22. R. Hudson, A. Riviere, C. M. Cirtiu, K. L. Luska and A. Moores, *Chem. Commun.*, 2012, 48, 3360-3362.
23. S. Peng and S. Sun, *Angew. Chem. Int. Ed.*, 2007, 46, 4155–4158.
24. J. Zeng, Q. Zhang, J. Chen and Y. Xia, *Nano Lett.*, 2009, 10, 30-35.

ChemComm Accepted Manuscript

25. K. Cheng, S. Peng, C. J. Xu and S. H. Sun, *J. Am. Chem. Soc.*, 2009, 131, 10637-10644.
26. K. Cheng and S. H. Sun, *Nano Today*, 2010, 5, 183-196.

1